

# Effects of co-doping nitrogen and germanium on dislocation gliding in Czochralski silicon: Implication for improving mechanical strength

Cite as: J. Appl. Phys. 128, 235105 (2020); doi: 10.1063/5.0029813

Submitted: 16 September 2020 · Accepted: 1 December 2020 ·

Published Online: 17 December 2020



Yuxin Sun, Wu Lan, Tong Zhao, Jianjiang Zhao, Defan Wu, Xiangyang Ma,<sup>a)</sup> and Deren Yang<sup>a)</sup>

## AFFILIATIONS

State Key Laboratory of Silicon Materials and College of Materials Science and Engineering, Zhejiang University, Hangzhou 310027, People's Republic of China

<sup>a)</sup>Authors to whom correspondence should be addressed: [mxyong@zju.edu.cn](mailto:mxyong@zju.edu.cn) and [mseyang@zju.edu.cn](mailto:mseyang@zju.edu.cn)

## ABSTRACT

Improving the mechanical strength of Czochralski (CZ) silicon is of significance for increasing the manufacturing yield of integrated circuits. In this work, we have comparatively investigated the dislocation gliding behaviors in the conventional CZ silicon, nitrogen (N)-doped CZ silicon, germanium (Ge)-doped CZ silicon as well as Ge and N co-doped CZ silicon subjected to the indentations for 30 min at different temperatures in the range of 850–1050 °C with an interval of 50 °C. It is found that the suppressing effect of N-doping on the dislocation gliding is strongest at 950 °C and becomes slightly weakened at higher temperatures, while Ge-doping does not exert a remarkable suppressing effect on the dislocation gliding until the temperature exceeds 950 °C. The co-doping of N and Ge impurities takes both advantages of N- and Ge-doping to suppress the dislocation gliding in CZ silicon at the aforementioned temperatures. More importantly, at 1000 and 1050 °C that are the typical processing temperatures for integrated circuits, the N and Ge co-doping exhibits a stronger suppressing effect on the dislocation gliding in CZ silicon than the single Ge- or N-doping. This indicates that the mechanical strength of CZ silicon in terms of the resistance of dislocation gliding at a high temperature can be further improved by co-doping Ge and N impurities. It is believed that the N-doping can result in the formation of larger grown-in oxygen precipitates and N–O complex-related pinning agents within the dislocations to suppress the dislocation gliding at 850–1050 °C with the strongest suppressing effect at 950 °C, while the suppressing effect of Ge-doping on the dislocation gliding at the temperatures exceeding 950 °C is tentatively ascribed to the formation of Ge–O complexes near the front of the dislocation lines.

Published under license by AIP Publishing. <https://doi.org/10.1063/5.0029813>

## I. INTRODUCTION

As the most widely used base material for manufacturing integrated circuits (ICs), Czochralski (CZ) silicon exhibits much better applicability than float-zone (FZ) silicon. This is due not only to the technical feasibility of the CZ method to grow large diameter (>200 mm) silicon crystals but also to the better mechanical strength of CZ silicon against dislocation generation and gliding. Oxygen, as the primary impurity unintentionally doped into CZ silicon, is well known to exert strong pinning of dislocations, thus improving the mechanical strength.<sup>1–5</sup> With an increasingly larger diameter, the dislocation generation and gliding become more readily in CZ silicon wafers because of self-weighting.<sup>6–9</sup> Therefore, how to further improve the mechanical strength of CZ silicon

through intentional doping of other electrically inactive impurities has been a matter of concern over the past decades.

The impurity of nitrogen (N), despite its low solubility in silicon, exhibits remarkable suppression of dislocation generation and gliding under certain circumstances.<sup>10–17</sup> Through the tensile tests at 800 or 900 °C, Sumino *et al.* found that the magnitude of upper yield stress was increased in pre-dislocated FZ silicon crystal due to N-doping.<sup>10</sup> They believed that the nitrogen atoms congregated at dislocation core to form clusters or complexes, which have a high energy of interaction with the dislocation, thus exhibiting a strong locking effect. Mezhenyi *et al.* revealed that the N-doping with the concentrations exceeding  $1.6 \times 10^{14} \text{ cm}^{-3}$  in CZ silicon resulted in a considerable increase in the critical stress for the onset of dislocation gliding from the indentation at temperatures ranging

from 500 to 800 °C.<sup>11,15</sup> They suggested that the N-doping promoted the formation of oxygen precipitates that immobilized the dislocations. Yonenaga *et al.* investigated the effect of N-doping with concentrations up to  $6 \times 10^{15} \text{ cm}^{-3}$  on the dislocation behavior in CZ silicon in the temperature range of 650–950 °C by means of three-point bending.<sup>12</sup> They found that the immobilization of dislocations due to the N-doping was effective at temperatures up to 900 °C, and the more effective immobilization occurs at relatively low temperatures of 650–750 °C, which was attributed to the formation of pinning agents along a single dislocation resulting from the cooperation of N and O impurities. Contrarily, the immobilization of dislocations became weaker in the N-doped CZ silicon than in the N-free CZ silicon at temperatures higher than 900 °C, which was tentatively ascribed to the rapid segregation of N impurity along the dislocations.<sup>12</sup>

Germanium (Ge)-doping was also used in an attempt to improve the mechanical strength of CZ silicon.<sup>18–23</sup> Yonenaga *et al.* measured the critical shear stress ( $\tau_c$ ) of dislocation generation at 800 °C by means of three-point bending. The  $\tau_c$  of dislocation generation for the CZ silicon doped with Ge impurity at  $6\text{--}9 \times 10^{19} \text{ cm}^{-3}$  was found to be nearly the same as that for the Ge-free CZ silicon. As the Ge concentration was above  $1.0 \times 10^{20} \text{ cm}^{-3}$ , the  $\tau_c$  of dislocation generation was slightly increased.<sup>18,19</sup> Fukuda *et al.* reported that the dislocation rosette size at 900 °C was independent on the Ge concentration up to  $3 \times 10^{20} \text{ cm}^{-3}$  in the oxygen-free silicon epitaxial layer, indicating that the Ge atoms themselves hardly influence the dislocation behavior,<sup>20</sup> while reporting that the dislocation rosette size in CZ silicon decreased in a manner with increasing Ge concentration from  $6 \times 10^{19}$  to  $3.7 \times 10^{20} \text{ cm}^{-3}$ . Such improved mechanical strength was ascribed to the immobilization of dislocations, which is caused by the oxygen atoms located next to the Ge ones. While the aforementioned reports addressed the Ge-doping effect on the dislocation behavior at temperatures up to 900 °C, Chen *et al.* reported that the Ge-doping with concentrations higher than  $10^{18} \text{ cm}^{-3}$  decreased the dislocation rosette sizes in CZ silicon annealed at 1100 °C.<sup>21</sup> Of practical significance, Taishi *et al.* realized the growth of dislocation-free CZ silicon crystal using a  $9 \times 10^{19} \text{ cm}^{-3}$  Ge-doped silicon seed without Dash necking process.<sup>22</sup> This result indicated that the heavy Ge-doping significantly suppressed the gliding of dislocations induced by the thermal shock arising from the silicon melt.

During the fabrication of ICs, quite a few processes such as thermal oxidation, the embedding of materials with thermal expansion coefficients different from that of silicon and deposition of films with intrinsic stress lead to the development of stress in the silicon substrate. Given enough stress, the dislocations will occur in the silicon substrate, resulting in charge leakage and electrical shorting between elements in ICs.<sup>24–26</sup> With decreasing feature size of ICs, the packing density of circuits on a chip increases and the device dimensions are reduced. These two trends lead to the processes in which stress levels increase, thus resulting in more probability of generating dislocations.<sup>24</sup> Although the processing conditions can be optimized for the fabrication of ICs to alleviate the stress-induced dislocations, the further strengthening of the silicon substrate is a fundamental strategy which can, in turn, broaden the process window for minimizing the likelihood of dislocation generation. Moreover, the manufacturing of ICs will

probably move into 450 mm CZ silicon wafer generation in the future. Due to the significant increase in self-weight, the dislocation generation and gliding are much more readily in 450 mm silicon wafers than in 300 mm and smaller diameter silicon wafers.<sup>8,9</sup> Then, the further improvement of mechanical strength is vital to 450 mm silicon wafers.

In this work, we have attempted co-doping dual impurities of N and Ge into CZ silicon to achieve better mechanical strength than that of singly N- or Ge-doped CZ silicon. In order to evaluate the mechanical strength of silicon at elevated temperatures, we have developed an apparatus for implementing indentation on silicon at 800–1050 °C for a length of time to enable dislocation gliding. Through comparing the dislocation rosette sizes in the specimens of conventional CZ silicon, N-doped CZ (NCZ) silicon, Ge-doped CZ (GCZ) silicon as well as N and Ge co-doped CZ (GNCZ) silicon subjected to the indentation under the same conditions in the aforementioned apparatus, we have verified the substantial improvement in the mechanical strength of CZ silicon due to the N and Ge co-doping. Furthermore, the mechanisms of N- and Ge-doping underlying the improved mechanical strength have been addressed.

## II. EXPERIMENTAL DETAILS

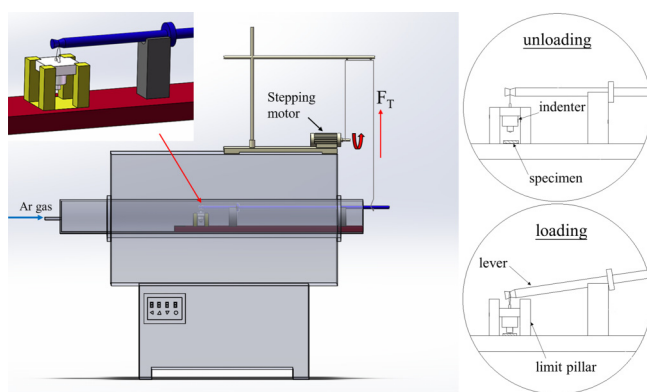
Seven 150 mm diameter,  $\langle 100 \rangle$ -oriented, lightly phosphorus-doped ( $10^{14} \text{ cm}^{-3}$  levels) CZ silicon crystal ingots were grown under nearly the same pulling conditions. Besides the conventional CZ silicon ingot without intentional doping of other impurities, there were two ingots doped with Ge at two levels of concentration (denoted as GCZ-1 and GCZ-2), two ingots doped with N at two levels of concentration (denoted as NCZ-1 and NCZ-2), and two ingots co-doped with N and Ge at two levels of concentration (denoted as GNCZ-1 and GNCZ-2). From the same position of each ingot, one  $\sim 1$  mm thick wafer was sliced. Table I shows the interstitial oxygen concentration ( $[O_i]$ ), N concentration ( $[N]$ ), or Ge concentration ( $[Ge]$ ) for the aforementioned seven silicon wafers. Herein, CZ silicon wafer is used as the control, GCZ-1, NCZ-1, and GNCZ-1 silicon wafers with relatively lower impurity concentrations are categorized into group 1, while GCZ-2, NCZ-2, and GNCZ-2 silicon wafers with higher impurity concentrations into group 2. The  $[O_i]$ s were measured by a Bruker Vertex 77V Fourier transform infrared (FTIR) spectroscope with the conversion

TABLE I. Concentrations of impurities in the silicon wafers used.

Wafer		Impurity		
		$[Ge]$ ( $10^{19} \text{ cm}^{-3}$ )	$[N]$ ( $10^{14} \text{ cm}^{-3}$ )	$[O_i]$ ( $10^{17} \text{ cm}^{-3}$ )
Control	CZ	/	/	7.9
Group 1	GCZ-1	2.8	/	8.1
	NCZ-1	/	2.1	8.1
	GNCZ-1	2.5	2.7	7.8
	GCZ-2	11.0	/	8.2
Group 2	NCZ-2	/	9.0	8.1
	GNCZ-2	9.9	7.5	8.1

coefficient of  $3.14 \times 10^{17} \text{ cm}^{-2}$  (ASTM F 131-83 standard). The [N]s and [Ge]s were measured by secondary ion mass spectroscopy. In either group, the GNCZ wafer contains the [N] and [Ge] comparable with that of NCZ or GCZ wafer. Note that the substitutional carbon concentration in each silicon wafer is below the detection limit of FTIR spectroscopy. A few of specimens sized in  $\sim 1 \times 1 \text{ cm}^2$  were cleaved from each silicon wafer. Each specimen was mechano-chemically polished by a Struers Tegraforce-5 system, followed with the chemical polishing in a HF: HNO<sub>3</sub> (1: 3 in volume ratio) reagent at  $\sim 30^\circ\text{C}$ , resulting in a final thickness of  $\sim 700 \mu\text{m}$ . In order to investigate the dislocation gliding behaviors in the aforementioned silicon wafers, each specimen was subjected to the indentation at an elevated temperature for 30 min, performed in a home-made apparatus, which will be detailedly described in the following.

Figure 1 shows the schematic diagram for the home-made indentation apparatus which consists primarily of a quartz-tube furnace and an indentation unit. The indentation unit is schematically illustrated in the top-left inset of the figure. In this indentation unit, the platform for placing specimen is made of fused quartz and the indenter with a tip of semi-sphere shape is made of alumina ceramics. The reason why the indenter is not made of diamond is that the air could enter into the quartz tube, which will result in the oxidation of diamond. Prior to the indentation, the specimen was placed onto the platform of the indentation unit. Subsequently, the indentation unit was loaded into the quartz-tube furnace. Under the argon ambient with a flowing rate of 5 l/min, the indentation unit was heated to a designated temperature with a subsequent 10 min dwelling to ensure the thermal equilibrium. For imposing the indentation, the indenter was slowly descended onto the silicon specimen through lowering the left end of the lever by a stepping motor, as shown in the bottom-right inset of Fig. 1. Because the connection between the indenter and the lever is soft and the friction forces between the indenter and the four limit pillars are negligible, the weight of the indenter ( $\sim 0.47 \text{ N}$ ) can be



**FIG. 1.** Schematic diagram for the indentation apparatus consisting primarily of a quartz-tube furnace and an indentation unit. The top-left inset schematically shows the indentation unit. The loading or unloading of indenter is illustrated in the bottom- or upper-right inset.

regarded as the indentation loading. Upon finishing the indentation, the indenter was lifted by raising the left end of the lever by the stepping motor, as shown in the upper-right inset of Fig. 1. In this work, the aforementioned indentation at the elevated temperature was performed at 850, 900, 950, 1000, or  $1050^\circ\text{C}$  for 30 min. At a given temperature, five indentations were imposed on each specimen.

In order to delineate the gliding of dislocations initiating from the indentation impression, the specimen indented at a given temperature was preferentially etched in Yang-1 etchant [CrO<sub>3</sub> (0.5 mol/l): HF (49%) = 1:1 in volume ratio] at  $30^\circ\text{C}$  for 10 min, followed with the observation under an Olympus MX-50 optical microscope (OM) equipped with a CCD camera. Moreover, to learn the dislocation behavior around the indentation impression at a microscopic scale, a HITACHI FB2200 focused ion beam (FIB) system was employed to pick up a micrometer-sized slice at the periphery of indentation impression, which was imposed on the investigated silicon specimen according to the procedure as described above. Such a slice was then thinned to  $\sim 100 \text{ nm}$  to act as the specimen for transmission electron microscope (TEM) characterization, which was implemented on a FEI Tecnai G2 F20 S system with the maximum accelerating voltage of 200 kV.

### III. RESULTS

#### A. Comparison of dislocation rosette sizes

Figure 2(a) shows a typical OM image obtained with the differential interference (DIF) mode for the indentation impression imposed on a CZ silicon specimen at  $1000^\circ\text{C}$  for 30 min. As can be seen, the indentation impression is seriously deformed. This indicates that the dislocation multiplication occurs significantly under the indenter, leading to the plastic deformation. Note that there are stripes distributing along with four  $[110]$  directions initiating from the indentation impression, which is actually indicative of dislocation gliding. The specimen of Fig. 2(a) was preferentially etched in Yang-1 etchant, followed with the OM observation. The obtained OM image is shown in Fig. 2(b). As seen, the dislocation gliding along the four  $[110]$  directions initiating from the indentation impression forms a so-called “rosette.”<sup>27</sup> It is understandable that the dislocations are firstly generated under the indenter and then glide along the four  $[110]$  directions, driven by the shear stresses originated from the indenter. Intuitively, the indenter imposed on the silicon specimen creates a stable shear stress field at a given temperature with the shear stresses decreasing radially from the indenter tip. The dislocations cease to glide at the point where the shear stress is equal to the critical shear stress ( $\tau_c$ ) for the dislocation gliding at a given temperature, thus resulting in a specific rosette size.<sup>28</sup> Qualitatively, the smaller rosette size corresponds to the larger  $\tau_c$ . As shown in Fig. 2(b),  $a_1$  and  $a_2$  denote the lengths of the dislocation arms in the horizontal and vertical directions, respectively. In this work, the dislocation rosette size ( $S$ ) is defined as  $S = (a_1 + a_2)/4$ .

Figure 3 shows the dislocation rosette sizes for the two groups of specimens subjected to the indentations at  $850$ – $1050^\circ\text{C}$  for 30 min. Herein, for each data point which is derived from five indentation rosettes, the dislocation rosette size refers to the mean value and the error bar represents the standard deviation. As can

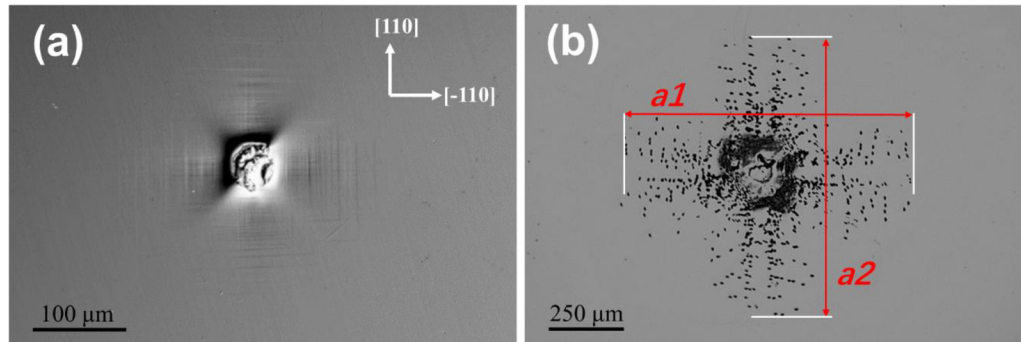


**FIG. 2.** (a) DIF-mode OM image of the indentation impression imposed on a CZ silicon specimen at 1000 °C for 30 min and (b) OM image for the specimen of (a) after the preferential etching in Yang 1 etchant.

be seen, the dislocation rosette size increases with the indentation temperature. This is due to that  $\tau_c$  for dislocation gliding decreases with increasing temperature. In each case, the dislocation rosette size of the CZ silicon specimen is the largest. By the way, it should be mentioned that the indentation at 800 °C for 30 min just leads to an indentation impression without appreciable dislocation gliding. With the indentation at 850, 900, or 950 °C, the dislocation rosette sizes of GCZ silicon specimens are quite close to that of the CZ silicon specimen, while the NCZ silicon specimens have much smaller dislocation rosette sizes than the CZ counterpart. Moreover, the GNCZ and NCZ silicon specimens possess almost the same dislocation rosette size. The aforementioned results indicate that the Ge-doping hardly exhibits the suppressing effect on the dislocation gliding at 850–950 °C, forming a striking contrast to the case of N-doping. It is, however, not the case when the indentation is imposed at a higher temperature of 1000 or 1050 °C. As can be seen from Fig. 3, with the indentation at 1000 or 1050 °C, the dislocation rosette sizes of GCZ silicon specimens are much smaller than that of CZ silicon specimen, indicating that the Ge-doping remarkably suppresses the dislocation gliding at such two elevated temperatures. Regarding the NCZ silicon specimens,

their dislocation rosette sizes are much smaller than that of the CZ counterpart all the same. Noteworthy, the dislocation rosette sizes are smaller in the GCZ silicon specimens than in the NCZ counterparts at 1050 °C. Moreover, as shown in Fig. 3, the dislocation rosette sizes of GNCZ silicon specimens are slightly smaller than those of GCZ counterparts at 1050 °C. This means that, for GNCZ silicon, the Ge-doping dominates over the N-doping to suppress the dislocation gliding at 1050 °C. At 1000 °C, the NCZ and GCZ silicon specimens have nearly the same dislocation rosette size that is much smaller than that of the CZ silicon specimen, while the GNCZ silicon specimens have much smaller dislocation rosette sizes than both the GCZ and NCZ counterparts. Therefore, it can be believed that the N and Ge impurities co-act to suppress the dislocation gliding at 1000 °C.

To quantitatively investigate the suppressing effect of N- or/and Ge-doping on the dislocation gliding in the CZ silicon, the difference percentages of the dislocation rosette size of control CZ silicon specimen relative to those of GCZ, NCZ, and GNCZ silicon specimens are derived from Fig. 3 with the results as given in Table II. As can be seen for GCZ silicon, the suppressing effect is very limited at 850–950 °C and becomes considerably strong at

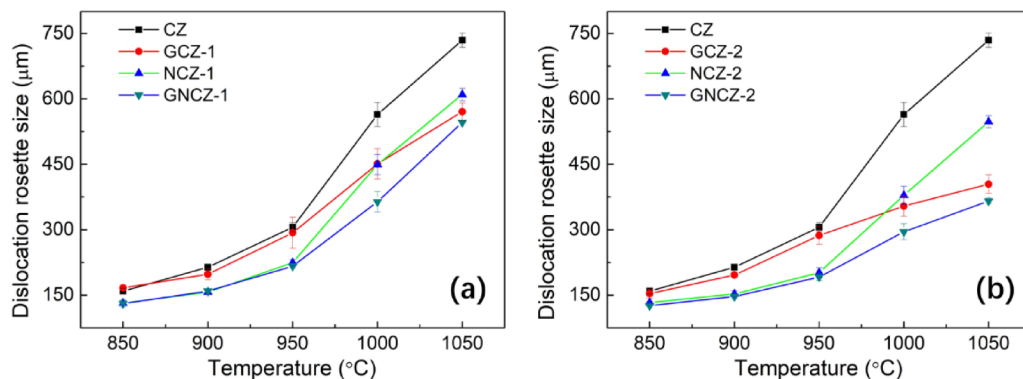


**FIG. 3.** The dislocation rosette sizes of different specimens subjected to the indentations at 850, 900, 950, 1000, or 1050 °C for 30 min: (a) group 1 and (b) group 2. The control CZ silicon specimen is included in either group.



1000–1050 °C. While for NCZ silicon, the suppressing effect becomes ever-stronger with temperature increasing from 850 to 950 °C and then becomes weakened in a manner at higher temperatures of 1000 and 1050 °C. Regarding GNCZ silicon, the suppression of dislocation gliding at 850–950 °C is dominated by the N-doping, while the weakened suppressing effect of N-doping on the dislocation gliding at 1000 or 1050 °C can be compensated by the enhanced suppressing effect of Ge-doping. Overall, the suppressing effect on the dislocation gliding in GNCZ silicon becomes progressively stronger with increasing temperatures, as shown in Table II. One exception appears for GNCZ-1 silicon at 1050 °C, which is due to the relatively low Ge concentration. In a word, the complementary advantages of N- and Ge-doping for improving the mechanical strength in terms of the resistance of dislocation gliding are well combined in GNCZ silicon. As a result, the mechanical strength of GNCZ silicon is better than that of either NCZ or GCZ silicon at elevated temperatures.

### B. TEM characterization

Figures 4(a) and 4(b) show the OM images of the indentation impressions imposed at 900 °C for 30 min on the CZ and GCZ-2 silicon specimens, respectively. As can be seen, there is no striking difference between the two indentation impressions, which illustrate no obvious deformations. Note that the morphologies of these two indentation impressions are quite different from that of the indentation impression imposed at 1000 °C for 30 min, which is shown in Fig. 1(a). Understandably, the indentation at 900 °C brings about much weaker plastic deformation than that at 1000 °C. Figures 4(c) and 4(d) show the cross-sectional TEM images of the dislocations formed at the peripheries of the indentation impressions as shown in Figs. 4(a) and 4(b), respectively. Actually, the dislocations were not readily found during the TEM observation, indicating that the dislocation densities in both the CZ and GCZ-2 silicon specimens are quite low. The statistical analysis on ten dislocation lines (not all shown herein) derives that the average dislocation lengths are  $\sim 0.30$  and  $0.28 \mu\text{m}$  in the CZ and GCZ-2 specimens, respectively. Therefore, it can be believed that the Ge-doping hardly suppresses the dislocation gliding at 900 °C. This result, from the point of microscopic view, verifies that the

**TABLE II.** The difference percentages (%) of the dislocation rosette size of control CZ silicon specimen relative to those of GCZ, NCZ and GNCZ silicon specimens, derived from Fig. 3. Taking a NCZ-1 silicon specimen at a given temperature, for example, the difference percentage given in the table is defined as: (dislocation rosette size of CZ–dislocation rosette size of NCZ-1)  $\div$  dislocation rosette size of CZ  $\times 100\%$

Specimen	Temperature				
	850 °C	900 °C	950 °C	1000 °C	1050 °C
GCZ-1	−4.6	7.5	4.2	20.1	24.6
GCZ-2	3.8	8.3	6.2	37.2	44.9
NCZ-1	17.4	26.7	26.5	20.3	17.0
NCZ-2	16.6	28.6	34.0	32.8	25.4
GNCZ-1	17.9	25.5	29.2	35.5	25.7

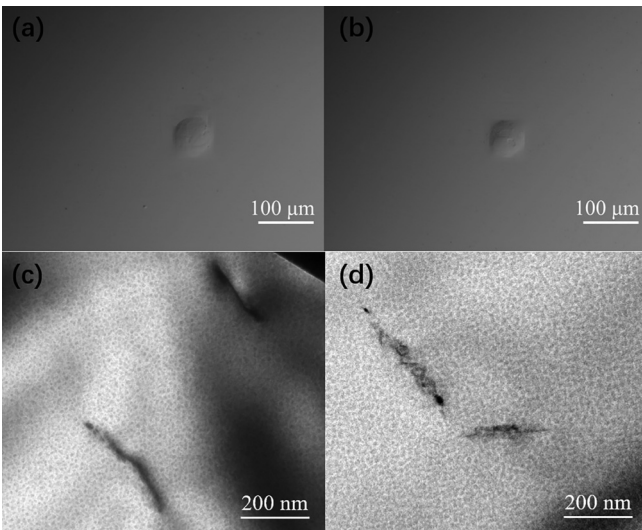


**FIG. 4.** OM images of the indentation impressions imposed at 900 °C for 30 min on (a) CZ and (b) GCZ-2 silicon specimens. Cross-sectional TEM images of the dislocations formed at the peripheries of indentation impressions imposed at 900 °C for 30 min on (c) CZ and (d) GCZ-2 silicon specimens with the view-plan projected to the  $\langle 011 \rangle$  direction.

Ge-doping hardly affects the dislocation gliding at the relatively low temperatures ranging from 850 to 950 °C, which has been revealed in Fig. 3. Combining with the previously reported results,<sup>18–20</sup> a consensus can be reached that the Ge-doping with a concentration lower than  $10^{20} \text{ cm}^{-3}$  hardly suppresses the dislocation gliding in CZ silicon at temperatures below 1000 °C.

Figure 5 shows the cross-sectional TEM images of the dislocations formed at the peripheries of the indentation impressions

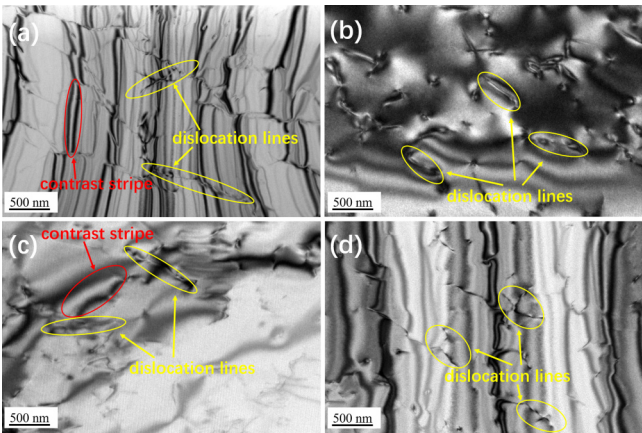


**FIG. 5.** Cross-sectional TEM images of the dislocations formed at the peripheries of indentation impressions on (a) CZ, (b) GCZ-2, (c) NCZ-2, and (d) GNCZ-2 silicon specimens imposed at 1000 °C for 30 min with the view-plan projected along the  $\langle 011 \rangle$  direction.

**TABLE III.** The number and length of dislocations in CZ, GCZ-2, NCZ-2, or GNCZ-2 silicon specimen, derived from the TEM images shown in Fig. 5.

Specimen	CZ	NCZ-2	GCZ-2	GNCZ-2
Number	44	48	57	64
Average length ( $\mu\text{m}$ )	0.45	0.40	0.26	0.22
Standard deviation ( $\mu\text{m}$ )	0.24	0.17	0.15	0.10

imposed at 1000 °C for 30 min on the CZ, GCZ-2, NCZ-2, and GNCZ-2 silicon specimens. Herein, just the TEM image containing the largest number of dislocations is selected for each specimen. Therefore, it seems reasonable to compare the dislocation behaviors in the aforementioned specimens using the TEM images as shown in Fig. 5. Besides the dislocation lines, quite a few contrast stripes appear in each TEM image due to the distortion of specimens. Actually, the FIB thinning process also affects the status of distortion. The details of such distortion are out of concern in this work. Table III lists the number and length of dislocations observed in each TEM image as shown in Fig. 5. As can be seen, the numbers and lengths of dislocations are comparable for the CZ and NCZ-2 silicon specimens. This is also the case for the GCZ-2 and GNCZ-2 silicon specimens. Note that the dislocations in the GCZ-2 and GNCZ-2 silicon specimens are much more but much shorter than those in the CZ and NCZ-2 counterparts. Evidently, the aforementioned results indicate that the N-doping slightly affects but the Ge-doping significantly suppresses the dislocation gliding at the periphery of indentation impression imposed at 1000 °C. This will be tentatively explained in the following. As for the fact that much more dislocations are generated in the GCZ-2 and GNCZ-2 silicon specimens, it is actually the expenditure on the shorter dislocation lengths for releasing the stresses that are nearly the same in the CZ and NCZ-2 counterparts.

#### IV. DISCUSSION

In the above, in terms of dislocation rosette size, it has been revealed that the N-doping exhibits the suppressing effect on the dislocation gliding in the temperature range of 850–1050 °C, while the Ge-doping does not take effect to suppress the dislocation gliding until the temperature exceeds 950 °C. The TEM observation at the periphery of the indentation impression reveals that the Ge-doping can impede the dislocation gliding at 1000 °C even under high shear stress, which is quite the contrary to the scenarios of lower temperatures. Regarding the N-doping, the TEM characterization indicates that it hardly suppresses the dislocation gliding at the periphery of the indentation impression imposed at 1000 °C. In the following, the mechanisms underlying the effects of N- and Ge-doping on the dislocation gliding will be tentatively explored.

##### A. N-doping

As revealed in Fig. 3, the N-doping remarkably suppresses the dislocation gliding, thus resulting in much smaller rosette sizes in the NCZ and GNCZ silicon specimens. The mechanism underlying the suppression of dislocation gliding due to the N-doping has been addressed previously.<sup>11–13</sup> The energy of interaction between a

single N atom and a dislocation is too small to effectively immobilize the dislocation.<sup>12,29</sup> It is well known that the dislocations are capable of gettering the in-diffusing impurities.<sup>30</sup> Namely, the dislocations can accommodate the impurity atoms or offer the sites for reaction/interaction between different impurities. It is generally believed that the N and O atoms gettering into a single dislocation can interact to form so-called N–O complexes,<sup>31–33</sup> which act as the “pinning agents” at the dislocation core. Under certain circumstances with sufficient annealing time, tiny oxide precipitates that can form through the heterogeneous nucleation based on the N–O complexes may also immobilize the dislocation.<sup>11–13</sup> In view of the previous reports,<sup>34,35</sup> it is known that the N–O complexes of different compositions can form in a wide temperature range of ~650–1100 °C. In this work, the indentation time was only 30 min so that the tiny oxide precipitates heterogeneously nucleating on the N–O complexes were hardly generated. Alternatively, the oxygen-related clusters initiating from the N–O complexes could be generated to immobilize the dislocation. Although what exactly immobilizes the dislocation in NCZ silicon is unknown, it is definite that the interaction between N and O impurities, thus, forming N–O complex-related pinning agents within the dislocation core plays an important role in the suppression of dislocation gliding. On the other hand, it has been reported that NCZ silicon usually possesses much larger grown-in oxide precipitates and can be stable up to 900 °C, in comparison with those in the conventional CZ silicon.<sup>36</sup> Such grown-in oxide precipitates can survive and grow up to suppress the dislocation gliding in NCZ silicon as the temperature is lower than 950 °C. Starting from 1000 °C, the stability of grown-in oxide precipitates in NCZ silicon markedly drops and the density of surviving oxide precipitates is considerably low, resulting in a weakened suppression effect.

In this work, the dislocation generation and subsequent gliding are driven by the shear stresses induced by the indenter. In this context, the shear stresses decrease progressively along with the dislocation gliding directions. It should be pointed out that the aforementioned suppression of the dislocation gliding due to the N–O complex-related pinning agents actually occurs in the regions that are sufficiently far away from the indentation impression. Therein, the shear stresses caused by the indenter are small enough so that the dislocation gliding speed is considerably reduced. Moreover, the dislocation density is also significantly decreased. Consequently, the N and O atoms that gettering into a single dislocation are considerable, leading to forming enough N–O complex-related pinning agents to immobilize the dislocation. While in the regions nearby the indentation impression, the dislocation density is very high and the dislocation gliding is very rapid driven by the large shear stresses. In this case, the N–O complex-related pinning agents formed in a single dislocation are too few to exhibit a substantial locking effect. As revealed in Fig. 5 and Table III, the N-doping does not remarkably suppress the dislocation gliding at 1000 °C in the region nearby the indentation impression. Although the dislocations generated at the periphery of indentation impression imposed at 850–950 °C on the NCZ silicon specimen have not been investigated by means of TEM, according to the aforementioned analysis, it can be logically derived that the N-doping also exhibits no noticeable suppressing effect on the dislocation gliding nearby the indentation impression, where the shear stresses are

relatively large. Actually, in the previous reports,<sup>12,18</sup> it has been proved that the N-doping cannot suppress the dislocation gliding at 650–950 °C under large shear stresses.

As mentioned above, the suppressing effect of N-doping on the dislocation gliding becomes a little weakened as the temperature is increased to 1000 and 1050 °C. At such two elevated temperatures, the nitrogen diffusivities are considerably large.<sup>37</sup> Therefore, the amount of N atoms captured in a single dislocation is to a certain extent reduced. Moreover, the supersaturation of oxygen is lessened. In this context, the amount of N–O complex-related pinning agents in a single dislocation is somewhat reduced. Moreover, the surviving grown-in oxide precipitates are remarkably decreased in NCZ silicon at 1000 and 1050 °C. Such two factors as mentioned above result in a little weakened suppressing effect of N-doping on the dislocation gliding at 1000 and 1050 °C.

## B. Ge-doping

The Ge atoms incorporated into silicon crystal generally occupy the substitutional lattice sites with an atomic size ~4% larger than that of the silicon atom. In principle, the interaction between the Ge atoms and a single dislocation can occur through the elastic strain fields of the Ge atoms and dislocation. Nevertheless, the energy of such interaction is considerably small. It has been calculated that the interaction energy between a Ge atom and a single dislocation is only 0.25 eV at 730 °C.<sup>19</sup> Actually, the energy of interaction between an impurity atom and a single dislocation hardly exceeds 0.5 eV even for an impurity atom introducing a large misfit strain in a semiconductor crystal.<sup>29</sup> In a word, the misfit strain of substitutional Ge atoms in silicon lattice is quite small so that the energy of interaction of a single dislocation with individual Ge atoms through the strain fields results in no appreciable locking effect. On the other hand, the Ge concentration is lower than 0.2 at. % in the present GCZ silicon specimens. Moreover, the substitutional Ge atoms diffuse quite slowly in silicon even at high temperatures.<sup>38</sup> Therefore, the formation of a solute atmosphere that immobilizes the dislocations in the present GCZ silicon is thermodynamically unfavorable. Then, as for the reason why the Ge-doping suppresses the dislocation gliding at temperatures higher than 950 °C, as revealed in Figs. 3 and 5 as well as in Table III, it remains an open question. As will be described below, it is tentatively proposed that the Ge–O complexes can form ahead of a single dislocation at high temperatures, resulting in the suppression of dislocation gliding.

For the sake of elucidation, Fig. 6(a) shows the schematic diagram for a typical 60° dislocation of shuffle set in silicon lattice, and Fig. 6(b) shows the simplified model of Fig. 6(a) projected in the direction of  $\langle 110 \rangle$ .<sup>39</sup> As shown in Fig. 6(b), the extra half plane with an edge component brings about compressive strain in its surrounding while generating tensile strain around its front end. It is believed the energy of the dislocated system can be lowered by forming large-sized complexes or clusters in the region of tensile strain, where the silicon lattice is expanded.<sup>40</sup> Actually, the formation of Ge–O complexes is not energetically favorable in the perfect silicon lattice since the compressive stress will be generated when the  $O_i$  atoms aggregate around a substitutional Ge atom.<sup>41</sup> However, such compressive stress can be accommodated in the

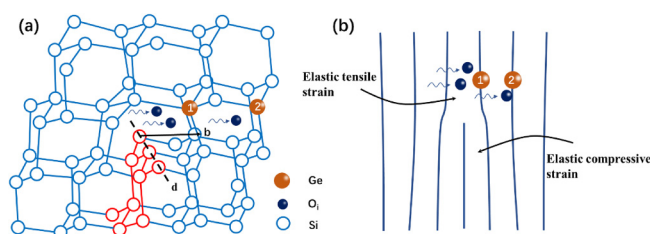


**FIG. 6.** (a) Schematic model of a “shuffle set” 60° dislocation in silicon lattice with the extra half plane denoted by red color. “d” is the dislocation line and “b” is the Burgers vector. The substitutional Ge and interstitial oxygen atoms are denoted by orange and blue filled balls, respectively. (b) The simplified schematic model of the “shuffle set” 60° dislocation projected in the direction of “d”/  $\langle 110 \rangle$  with elastic compressive and tensile strains in different regions.

tensile strained region in front of the dislocation. Therein, the formation of Ge–O complexes is, thus, facilitated. As schematically shown in Figs. 6(a) and 6(b), the Ge atom numbered with “1,” near the front of the dislocation, is a favorable site to form a Ge–O complex. Even for the Ge atom numbered with “2,” which is a little bit far away from the dislocation but is still located in the tensile stress field, is also a site to form a Ge–O complex. At high temperatures of 1000 and 1050 °C, the  $O_i$  atoms diffuse swiftly toward the Ge atoms at those specific sites as mentioned above. Moreover, the interaction between Ge and  $O_i$  atoms is energetically favorable. Consequently, the Ge–O complexes can form ahead of individual dislocations. Such Ge–O complexes can act as the pinning agents to suppress the dislocation gliding. At the relatively lower temperatures, the diffusivity of  $O_i$  atoms is much smaller, and the interaction between Ge and  $O_i$  atoms is less energetically favorable. In this case, the formation of Ge–O complexes ahead of a single dislocation is not remarkable. As a result, the dislocation gliding at the temperatures of 800–950 °C is hardly suppressed by the Ge-doping, as revealed in Fig. 3.

## C. N and Ge co-doping

As revealed in Fig. 3, co-doping of N and Ge into CZ silicon leads to the suppression of dislocation gliding at all the investigated temperatures. N-doping is primarily responsible for the dislocation immobilization at the temperatures not exceeding 950 °C through the formation of N–O complex-related pinning agents within the dislocation cores and larger grown-in nuclei of oxygen precipitate during the cooling process of crystal growth. However, the suppressing effect of N-doping is somewhat weakened at higher temperatures, the reason for which has been explained in the above. On the other hand, the Ge-doping exhibits an enhanced suppressing effect on the dislocation gliding at temperatures higher than 950 °C, which is supposed to be ascribed to the formation of Ge–O complexes near the front of the individual dislocation lines. Therefore, for GNCZ silicon, the complementary advantages of N- and Ge-doping are taken to suppress the dislocation gliding. Especially at 1000 °C, although the suppressing effect of N-doping is slightly weakened as compared to that at 950 °C, it is compensated by the remarkably enhanced suppressing effect of Ge-doping.



Therefore, the overall suppressing effect on the dislocation gliding reaches the strongest at 1000 °C for GNCZ silicon, as shown in Fig. 3 and Table II.

## V. CONCLUSION

We have comparatively investigated the dislocation gliding behaviors in the conventional CZ, N-doped CZ, Ge-doped CZ as well as N and Ge co-doped CZ silicon subjected to the indentation at the elevated temperatures ranging from 850 to 1050 °C. To this end, we have developed an indentation apparatus consisting primarily of a quartz-tube furnace and an indentation unit. It has been found that the N-doping exhibits the suppressing effect on the dislocation gliding at all the temperatures investigated, while the Ge-doping does not take effect to remarkably suppress the dislocation gliding until the temperature exceeds 950 °C. Moreover, the aforementioned suppressing effect of N-doping is found to be a little weakened beyond the temperature of 950 °C. Co-doping N and Ge impurities into CZ silicon can take full advantage of both N- and Ge-doping to improve the mechanical strength in terms of the resistance of dislocation gliding, especially at high temperatures such as 1000 and 1050 °C. It is believed that the N-doping can result in the formation of N-O complex-related pinning agents within the dislocation core to suppress the dislocation gliding at 850–1050 °C. Larger grown-in nuclei of oxygen precipitates also contribute to the suppression of dislocation gliding at relatively low temperatures. As for the mechanism underlying the suppressing effect of Ge-doping on the dislocation gliding at the temperatures exceeding 950 °C, it is supposed that the Ge-O complexes acting as the pinning agents can form near the front of a single dislocation, where the silicon lattice is expanded due to the elastic tensile strain. We believe that the present work gives an insight into the effects of Ge and N impurities on the mechanical strength of CZ silicon.

## ACKNOWLEDGMENTS

The author would like to thank the financial support from Natural Science Foundation of China (Grant Nos. 61674126, 51532007, and 61721005).

## DATA AVAILABILITY

The data that support the findings of this study are available from the corresponding authors upon reasonable request.

## REFERENCES

- <sup>1</sup>I. Yonenaga and K. Sumino, *Jpn. J. Appl. Phys.* **21**(1), 47–55 (1982).
- <sup>2</sup>S. M. Hu and W. J. Patrick, *J. Appl. Phys.* **46**(5), 1869–1874 (1975).
- <sup>3</sup>S. Senkader, K. Jurkschat, D. Gambaro, R. J. Falster, and P. R. Wilshaw, *Philos. Mag. A* **81**(3), 759–775 (2001).
- <sup>4</sup>Z. D. Zeng, X. Y. Ma, J. H. Chen, D. R. Yang, I. Ratschinski, F. Hevroth, and H. S. Leipner, *J. Cryst. Growth* **312**(2), 169–173 (2010).
- <sup>5</sup>Z. D. Zeng, J. H. Chen, Y. H. Zeng, X. G. Ma, and D. R. Yang, *J. Cryst. Growth* **324**(1), 93–97 (2011).
- <sup>6</sup>A. Fischer and G. Kissinger, *Appl. Phys. Lett.* **91**, 111911 (2007).
- <sup>7</sup>H. Shimizu and T. Aoshima, *Jpn. J. Appl. Phys.* **27**(12), 2315–2323 (1988).
- <sup>8</sup>M. Goldstein and M. Watanabe, *ECS Trans.* **16**(6), 3 (2008).
- <sup>9</sup>M. Watanabe, T. Fukuda, A. Ogura, Y. Kirino, and M. Kohno, *ECS Trans.* **2**, 155–165 (2006).
- <sup>10</sup>K. Sumino, I. Yonenaga, M. Imai, and T. Abe, *J. Appl. Phys.* **54**(9), 5016–5020 (1983).
- <sup>11</sup>M. V. Mezhenyi, M. G. Mil'vidskii, and V. Y. Reznik, *Phys. Solid State* **44**(7), 1278–1283 (2002).
- <sup>12</sup>I. Yonenaga, *J. Appl. Phys.* **98**(2), 023517 (2005).
- <sup>13</sup>H. M. Lu, D. R. Yang, L. B. Li, Z. Z. Ye, and D. L. Que, *Phys. Status Solidi A* **169**(2), 193–198 (1998).
- <sup>14</sup>J. D. Murphy, C. R. Alpass, A. Giannattasio, S. Senkader, R. J. Falster, and P. R. Wilshaw, *Nucl. Instrum. Meth. B* **253**(1–2), 113–117 (2006).
- <sup>15</sup>M. V. Mezhenyi, M. G. Mil'vidskii, and V. Y. Reznik, *J. Surf. Invest.* **3**(5), 747–751 (2009).
- <sup>16</sup>V. Orlov, H. Richter, A. Fischer, J. Reif, T. Müller, and R. Wahlich, *Mater. Sci. Semicon. Proc.* **5**(4–5), 403–407 (2002).
- <sup>17</sup>D. R. Yang, G. Wang, J. Xu, D. S. Li, D. L. Que, C. Funke, and H. J. Moeller, *Microelectron. Eng.* **66**(1–4), 345–351 (2003).
- <sup>18</sup>I. Yonenaga, *Mater. Sci. Eng. B* **124–125**, 293–296 (2005).
- <sup>19</sup>I. Yonenaga, T. Taishi, X. Huang, and K. Hoshikawa, *J. Appl. Phys.* **93**(1), 265–269 (2003).
- <sup>20</sup>T. Fukuda and A. Ohsawa, *Appl. Phys. Lett.* **60**(10), 1184–1186 (1992).
- <sup>21</sup>J. H. Chen, D. R. Yang, X. Y. Ma, Z. D. Zeng, D. X. Tian, L. B. Li, D. L. Que, and L. F. Gong, *J. Appl. Phys.* **103**(12), 123301 (2008).
- <sup>22</sup>T. Taishi, X. M. Huang, I. Yonenaga, and K. Hoshikawa, *Mater. Sci. Semicon. Proc.* **5**(4–5), 409–412 (2002).
- <sup>23</sup>I. Yonenaga, *Phys. Status Solidi A* **171**(1), 41–46 (1999).
- <sup>24</sup>P. M. Fahey, S. R. Mader, S. R. Stiffler, R. L. Mohler, J. D. Mis, and J. A. Slinkman, *IBM J. Res. Dev.* **36**(2), 158–182 (1992).
- <sup>25</sup>W. C. Hua, M. H. Lee, P. S. Chen, M. Tsai, and C. W. Liu, *IEEE Electr. Device Lett.* **26**(9), 667–669 (2005).
- <sup>26</sup>J. H. Park, S. W. Shin, S. W. Park, Y. T. Kong, D. J. Kim, M. S. Suh, S. C. Lee, N. Y. Kwak, C. D. Dong, D. W. Kim, G. I. Lee, O. J. Kwon, and H. S. Yang, *J. Electrochem. Soc.* **150**(7), G359–G364 (2003).
- <sup>27</sup>S. M. Hu, *J. Appl. Phys.* **46**(4), 1470–1472 (1975).
- <sup>28</sup>S. M. Hu, *Appl. Phys. Lett.* **31**(3), 139–141 (1977).
- <sup>29</sup>K. Sumino and I. Yonenaga, *Solid State Phenom.* **85–86**, 145–176 (2002).
- <sup>30</sup>D. Gilles, E. R. Weber, and S. Hahn, *Phys. Rev. Lett.* **64**(2), 196–199 (1990).
- <sup>31</sup>Q. Sun, K. H. Yao, H. C. Gatos, and J. Lagowski, *J. Appl. Phys.* **71**(8), 3760–3765 (1992).
- <sup>32</sup>V. D. Akhmetov, H. Richter, W. Seifert, O. Lysytskiy, R. Wahlich, T. Müller, and M. Reiche, *Eur. Phys. J. Appl. Phys.* **27**(1–3), 159–161 (2004).
- <sup>33</sup>G. Kissinger, U. Lambert, M. Weber, F. Bittersberger, T. Müller, H. Richter, and W. von Ammon, *Phys. Status Solidi A* **203**(4), 677–684 (2006).
- <sup>34</sup>W. von Ammon, R. Hölzl, J. Virbulis, E. Dornberger, R. Schmolke, and D. Gräf, *J. Cryst. Growth* **226**(1), 19–30 (2001).
- <sup>35</sup>D. R. Yang, X. Y. Ma, R. X. Fan, D. S. Li, J. X. Zhang, L. B. Li, D. L. Que, and K. Sumino, *Mater. Sci. Eng. B* **72**(2–3), 121–123 (2000).
- <sup>36</sup>G. Kissinger, T. Müller, A. Sattler, W. Häckl, M. Weber, U. Lambert, A. Huber, P. Krottenthaler, H. Richter, and W. Von Ammon, *Solid State Phenom.* **108–109**, 17–24 (2005).
- <sup>37</sup>T. Itoh and T. Abe, *Appl. Phys. Lett.* **53**(1), 39–41 (1988).
- <sup>38</sup>G. L. McVay and A. R. Ducharme, *J. Appl. Phys.* **44**(3), 1409–1410 (1973).
- <sup>39</sup>D. B. Holt and B. G. Yacobi, *Extended Defects in Semiconductors* (Cambridge University Press, 2007), p. 103.
- <sup>40</sup>J. P. Hirth and J. Lothe, *Theory of Dislocations*, 2nd ed. (Wiley, 1983), p. 656.
- <sup>41</sup>L. Wang and D. R. Yang, *Physica B* **404**(1), 58–60 (2009).